

Nature of Giant Pulses in Radio Pulsars

S. A. Petrova *

Institute of Radio Astronomy, 4, Chervonopraporna Str., Kharkov 61002, Ukraine

Abstract Formation of giant radio pulses is attributed to propagation effects in the plasma of pulsar magnetosphere. Induced scattering of radio waves by the plasma particles is found to lead to an efficient redistribution of the radio emission in frequency. With the steep spectrum of pulsar radiation, intensity transfer between the widely spaced frequencies may imply significant narrow-band amplification of the radiation. This may give rise to giant pulses. It is demonstrated that the statistics of giant pulse intensities observed can be reproduced if one take into account pulse-to-pulse fluctuations of the plasma number density and the original intensity. Polarization properties of the strongly amplified pulses, their location in the average pulse window and the origin of the nanostructure of giant pulses are discussed as well.

Key words: plasmas — pulsars: general — pulsars: individual: the Crab pulsar, PSR B1937+21 — scattering

1 MAIN FEATURES OF GIANT PULSES

The intensities of pulsar radio emission are known to vary from pulse to pulse. Typically they fluctuate within a few times the average and are believed to have Gaussian distribution. However, several pulsars exhibit a pronounced excess of strong pulses with a characteristic power-law distribution. These so-called giant pulses have intensities from a few dozens up to thousands times the average. At present there is no evidence for a break of the power-law tail at high intensities, so the observations of longer duration would reveal the pulses of even higher intensities. For low enough intensities, the role of noise is significant, and the observations do not give direct evidence as to whether giant pulses present a separate group or whether there is a smooth transition from normal to giant pulses. The power-law index of giant pulse distribution differs markedly for different pulsars ($\alpha \sim -1.5 \div -4$) and depends on radio frequency.

For a given pulsar, giant pulses constitute only a tiny fraction of the total of pulses, less than one per cent, and do not affect the average radio emission characteristics. The giant pulse profiles are characterized by a specific form, with fast rise and exponential decay, and are usually narrower than a normal pulse, the strongest ones tending to be the narrowest.

Giant pulses occur over a broad range of radio frequencies, from a few dozens MHz to a few GHz, but the normalized correlation bandwidth is not large, $\Delta\nu/\nu \sim n \cdot 0.1$. Typically giant pulses are not simultaneous out of this range (e.g. Popov & Stappers 2003). In case of the Crab pulsar, giant pulses are seen simultaneously over a broad frequency range (e.g. Sallmen et al. 1999), but their substructure is correlated only over the interval $\Delta\nu/\nu \lesssim 0.2$ (Eilek et al. 2002).

The presence of a substructure is one of the most prominent features of giant pulses. In the Crab pulsar, the giant pulses often consist of several components - the nanopulses - with timescales down to a few nanoseconds (Hankins et al. 2003). For another well-studied source of giant pulses, PSR B1937+21, there is also indirect evidence in favour of the nanostructure (Popov & Stappers 2003). Such tiny timescales imply tremendous brightness temperatures, $10^{37} - 10^{39}$ K (Hankins et al. 2003; Soglasnov et al. 2004), making nanopulses the brightest pulses in the Universe. Note that their energetics is only marginally consistent with the total energetics of pulsar magnetosphere and challenges our understanding of pulsar physics.

* E-mail: petrova@ira.kharkov.ua

Similarly to the giant pulses on the whole, the nanopulses are characterized by fast rise and exponential decay. The plot of the peak intensity versus width has a clear upper envelope, which corresponds to the constant integrated intensity of the nanopulses (Eilek et al. 2002).

On a qualitative level, apart from the scaling factors, the nanostructure of giant pulses looks very similar to the microstructure observed in the normal pulses, hinting at a similar origin. For a given pulsar, the microstructure shows a range of timescales with a definite upper cutoff. The most important property of the microstructure is that its characteristic timescale is exactly proportional to the pulsar period (Popov et al. 2002). The same trend can also be expected for the nanostructure of giant pulses: The period of PSR B1937+21 is about 20 times less than that of the Crab, so its nanopulses may be considerably shorter and, perhaps, just for this reason they still escape direct detection.

Another remarkable phenomenon relative to giant pulses is giant micro pulses found in the Vela and some other pulsars. Their peak intensities are up to 40 times the peak of the average profile and 130 times the average intensity at their longitude, and they also exhibit power-law statistics (Johnston et al. 2001). However, giant micropulses are so narrow that their integrated intensities are no more than a few times that of the average profile. It is interesting to note that at certain pulse longitudes, not active as to giant micro pulses, the intensity distribution also exhibits a tail, though weaker than the power-law tail of giant micro pulses. It appears consistent with log-normal statistics (Cairns et al. 2001). Thus, even at so called non-active longitudes, the radio emission of the Vela can be subject to amplification.

The results of polarization studies of giant pulses and relative phenomena are not very numerous. However, on the whole one can conclude that giant pulses, giant micro pulses and ordinary micro pulses are strongly polarized, much stronger than the typical normal pulses. In addition to high linear polarization, substantial amounts of circular polarization are sometimes present.

It has been noticed that among the known pulsars the first four sources of giant pulses have the largest magnetic field at the light cylinder, about a million Gauss. Moreover, this seems a single common feature of the sources, which have very different parameters and evolution histories. But the subsequent attempts to discover another giant pulse sources among the pulsars with the largest light cylinder magnetic field were not very fruitful. Instead, a couple of giant pulse sources were discovered at low enough frequencies, 40 & 111 MHz (PSR B1112+50 (Ershov & Kuzmin 2003) & B0031-07 (Kuzmin et al. 2004)). The giant pulses are very similar to the previously known, but the pulsars themselves have absolutely ordinary characteristics. An impression may arise that at low frequencies giant pulse phenomenon is so pronounced that no additional conditions, such as high light cylinder magnetic field, are necessary. At the same time, the actual frequency dependence of giant pulse efficiency remains ambiguous. PSR B1133+16 presents a counter example, showing an excess of strong pulses at high frequencies (Kramer et al. 2003).

Despite these recent detections, giant pulses are usually associated with the light cylinder. In particular, they are thought to be related to the pulsar high-energy emission, whose luminosities are also related to the light cylinder magnetic field. An idea of such a relation has even deeper roots. Normally, the energetics of radio emission is only a tiny fraction of the rotational energy loss of the pulsar and the role of radio emission processes in the global pulsar electrodynamics is negligible. However, as giant pulses show amplifications up to a few thousand and if they are sufficiently broad-band, their energetics may be at a level of global electrodynamic processes in pulsar magnetosphere. If any, the global electrodynamic changes during giant pulses should necessarily be reflected in the high-energy emission. However, the gamma-ray emission accompanying giant pulses of the Crab pulsar does not show any marked changes (Lundgren et al. 1995), the optical pulses are only 3% brighter (Shearer et al. 2003). In a word, the present high-energy data testify against global electrodynamic changes during giant pulses.

Moreover, the changes in the radio emission mechanism during giant pulses are also strongly restricted. In the Crab pulsar, the arrival times of giant pulses show no delay with respect to the normal ones, so that the emission region is the same (Lundgren et al. 1995). In PSR B1937+21, during giant pulses the radio emission beyond the narrow giant profile is also present and shows exactly the same characteristics as in the normal pulses. One can conclude that neither global electrodynamic processes nor special radio emission mechanism are necessary to explain giant pulse phenomenon. In this situation, it is reasonable to apply to propagation effects as the radio beam passes through the plasma of pulsar magnetosphere.

The peculiarities of giant pulse sources as to the average radio emission characteristics have not attracted much attention yet. But note that the largest known average radio luminosities and the steepest known radio spectra are both the attributes of giant pulse sources.

This is a rough observational picture of giant pulses and relative phenomena. It contains a lot of puzzles for theorists. The most important problems concern the source of energy supplying giant pulses, the mechanism of energy release providing the power-law statistics of giant pulse intensities, and the origin of the nanostructure. All these problems can be solved in terms of propagation effects in pulsar magnetosphere (Petrova 2004a, b).

2 INDUCED COMPTON SCATTERING IN PULSAR PLASMA

Pulsar magnetospheres are believed to contain the strongly magnetized electron-positron plasma, which streams along the open magnetic lines with ultrarelativistic velocities. The Lorentz-factors of the plasma $\gamma \sim 100$. The radio emission originates deep inside the open field line tube, and further on it should propagate through the plasma flow. The brightness temperatures of the normal pulsar radio emission are extremely high, $10^{25} - 10^{30}$ K, so that the induced scattering of radio photons off the plasma particles strongly dominates the spontaneous scattering and is expected to be efficient enough to have marked observational consequences.

Induced scattering is most efficient deep inside the magnetosphere, where the number density of the scattering plasma particles is the largest. In this region, the approximation of a superstrong magnetic field is valid: The radio frequency in the particle rest frame, $\omega' \equiv \omega\gamma(1 - \beta \cos \theta)$ (where β is the particle velocity in units of c and θ the photon tilt to the ambient magnetic field), is much less than the electron gyrofrequency, $\omega_H \equiv \frac{eB}{mc}$. Thus, we come to the problem of induced scattering in the superstrong magnetic field.

In the rest frame of the scattering particles, the photon frequency is almost unaltered in the scattering act. In the laboratory frame, this implies a certain relation between the photon frequencies and orientations in the initial and final states:

$$\omega_a \gamma (1 - \beta \cos \theta_a) = \omega_b \gamma (1 - \beta \cos \theta_b). \quad (1)$$

At a fixed frequency, the photons are concentrated into a narrow beam with the opening angle $\sim 1/\gamma$, but at substantially different frequencies the beams can have different orientations with respect to the local magnetic field. Although in the open field line tube the wavevector tilt to the magnetic field is not large, typically a few degrees, for different frequencies it can differ by a factor of a few. Correspondingly, induced scattering can transfer photons between widely spaced frequencies.

In the problem considered, the induced scattering transfers the photons mainly from the low-frequency state to the high-frequency one, with the total intensity at the two frequencies remaining constant (Petrova 2004a). With the steeply decreasing spectrum of pulsar radiation ($\alpha \sim -3$) and the frequency ratio of about 10, this may imply a drastic amplification of the higher-frequency intensity. Note that steeper radio spectra favour stronger amplification.

As long as the number of the low-frequency photons is not negligible, the high-frequency intensity grows exponentially, $I_a = I_a^{(0)} \exp(\Gamma)$. According to the numerical estimates, for the giant pulse sources, the optical depth to induced scattering is not large on average, $\langle \Gamma \rangle \sim 0.1$, i.e. on average this process is inefficient. Note that most of the observed pulses are indeed not giant. However, the scattering depth depends on the number density of the scattering particles, N , and the original intensity of radiation, $I^{(0)}$, which are believed to vary randomly from pulse to pulse. As from time to time they acquire the values more than three times the average, the optical depth becomes large and the intensity is strongly amplified. An exact mathematical treatment shows that if the plasma density and original intensity are Gaussian random variables, the final distribution of the strongly amplified intensities is close to the power law (Petrova 2004a).

3 OBSERVATIONAL CONSEQUENCES OF INDUCED SCATTERING IN PULSARS

3.1 Statistics of Intensity Amplification

The numerical simulations in the framework of the amplification model suggested, $I = I^{(0)} \exp(\Gamma) = I^{(0)} \exp \left[\langle \Gamma \rangle \left(\frac{I^{(0)}}{\langle I^{(0)} \rangle} \right) \left(\frac{N}{\langle N \rangle} \right) \right]$, allow to reproduce the observed intensity distributions of giant pulses.

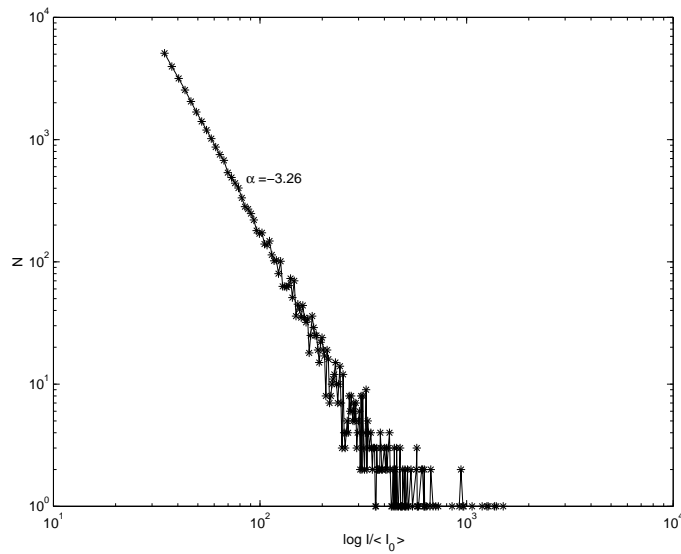


Fig. 1 Numerically simulated histogram of strongly amplified intensities, $I/\langle I_0 \rangle > 33\langle I_0 \rangle$.

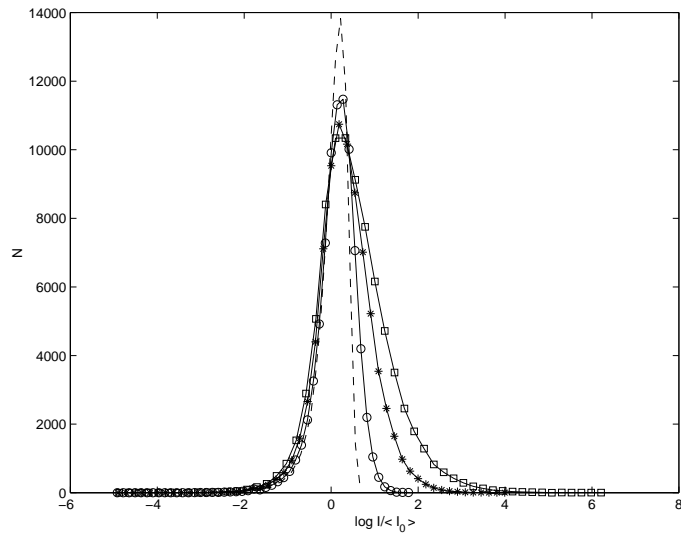


Fig. 2 Distribution of the logarithm of intensity for different average scattering depths. The circles, asterisks and squares correspond to $\langle \Gamma \rangle = 0.1, 0.3, \text{ and } 0.5$, respectively. The dotted line shows the original Gaussian intensity distribution.

Figure 1 shows the calculated histogram of strongly amplified intensities. It is close to the power law with the index $\alpha = -3.26$ and is similar to that observed for the Crab pulsar at the frequency of 800 MHz (Lundgren et al. 1995). The simulated histograms of the logarithm of intensity for a set of average scattering depths, $\langle \Gamma \rangle$, are presented in Figure 2. The curves appear close to the original Gaussian distribution, to the log-normal one and to the distribution with the power-law tail. All types of the histograms are indeed met in observations. In the Vela pulsar, at different pulse longitudes both the power-law and log-normal forms are met, testifying to the difference of the average scattering depth at different locations in the magnetosphere. Perhaps, just for this reason giant micro pulses are observed in this pulsar, instead of common giant pulses.

3.2 Basic Characteristics of Giant Pulses

The numerical estimates show that the average scattering depth is a function of a number of poorly known parameters (Petrova 2004a). The scattering efficiency is certainly proportional to the radio luminosity of a pulsar. Besides that, if the altitude of the scattering region is a certain fraction of the light cylinder, the scattering depth is also proportional to the light cylinder magnetic field. Note, however, that these trends can be substantially smeared by the implicit period and frequency dependencies of both the scattering geometry and the parameters of the plasma flow.

Keeping in mind the exponential form of the intensity growth, $I = \langle I_0 \rangle \exp(\Gamma)$, one can estimate the bandwidth of the amplified radiation as $\Delta\nu/\nu \sim 1/\Gamma$. Given that the maximum observed intensity amplification is about a few thousand times, the maximum scattering depth should be approximately 7. Hence, the estimated bandwidth of giant radiation roughly corresponds to the observed value of a few tenths. It should be noted, however, that the conditions for efficient beam-to-beam scattering can be satisfied simultaneously in a number of distinct regions in the open field line tube and different frequencies can be amplified independently. This may result in a broad-band activity of giant pulses similar to that observed in the Crab pulsar.

The width of a giant pulse can be roughly estimated as $w_{GP} \sim w/\Gamma$. Hence, giant pulses should indeed be somewhat narrower, with the strongest ones tending to be the narrowest, just as is really observed. Note, however, that the actual profiles of giant pulses should be determined by the location and geometry of the scattering region. In addition, giant pulses are strongly affected by interstellar scattering.

The suggested mechanism of giant pulses implies a strong polarization of the substantially amplified radiation. The ultrarelativistic strongly magnetized plasma of pulsars allows two non-damping natural waves - the ordinary and extraordinary ones, - which are linearly polarized in orthogonal directions. In general, the pulsar beam presents an incoherent superposition of the two types of waves and is partially depolarized. In the superstrong magnetic field, the process of induced scattering is efficient only for the ordinary waves. Hence, only the ordinary waves are amplified, whereas the fraction of the extraordinary ones in the total radio emission becomes so small that they cannot cause substantial depolarization. Thus, giant pulses should be strongly polarized and have the polarization of the ordinary waves, with the electric vector lying in the plane of the ambient magnetic field. The latter is still to be confirmed by observations.

3.3 Location of Giant Pulses in the Average Pulse Window

The necessary condition of giant amplification, i.e. substantial difference in the initial and final frequencies and orientations of the scattered waves (related by Equation (1)), can be valid only within some specific regions in the magnetosphere. In case of PSR B1937+21, which has the shortest known period, $P = 1.56$ ms, the rotational effect is very strong - even the stellar surface rotates at a speed of $0.1c$. The rays of different frequencies are thought to originate at different altitudes above the neutron star. (Higher frequencies are emitted deeper in the magnetosphere, where the plasma number density and the characteristic plasma frequency are larger.) The rays emitted at different altitudes propagate in the rotating magnetosphere and travel to the point of scattering for different time intervals. So they indeed come at substantially different angles.

An exact geometrical consideration leads to the conclusion that the necessary condition for giant amplification can be satisfied only for the rays emitted almost parallel to the magnetic axis in the laboratory frame (Petrova 2004a). Because of rotational aberration, the rays co-directed with the magnetic axis appear in the trailing part of the pulse profile. The giant pulses of PSR B1937+21 are indeed met within a narrow window at the trailing edge of the profile (e.g. Soglasnov et al. 2004). The observed time delay from the center of the average profile, $\tau \sim 60 \mu\text{s}$, translates to the aberration angle $\Delta\theta = 2\pi\tau/P \approx 0.2$, which seems quite realistic. Thus, it is very likely that the location of giant pulses in the profile of PSR B1937+21 coincides with the projection of the magnetic axis and is determined by the rotational effect.

As for the Crab pulsar, its period is about 20 times longer, and perhaps the rotational effect is too weak to provide the necessary geometrical condition of giant amplification. In this case, the necessary condition can be set up by the frequency-dependent refraction of radio waves. The location of the scattering region is then determined by the instantaneous distribution of the plasma in the open field line tube, which can markedly fluctuate, so that giant pulses can be met at different locations within the average profile.

4 ORIGIN OF THE MICRO/NANO STRUCTURE

The nanostructure of giant pulses and the relative phenomenon of microstructure in the normal pulsars can also be explained in terms of propagation effects in pulsar plasma.

The proportionality of the characteristic timescale of microstructure to pulsar period strongly supports the angular beaming model: The micro/nano pulses result from the inhomogeneity of the angular structure of pulsar beam, which manifests itself as the pulsar rotates. Then the angular scale of inhomogeneity is the same for all pulsars, while the difference of the timescales results simply from the difference in the velocity of rotation with respect to an observer, $\Delta\tau = P\Delta\theta/(2\pi)$. The angular scale of inhomogeneity is commonly associated with the opening angle of relativistically beamed radiation, $\Delta\theta \sim 1/\gamma$. However, this requires huge Lorentz-factors of the plasma, 10^4 for the microstructure and 10^7 for the nanostructure, while the modern theories of pair creation cascade in pulsars give the values $\gamma \sim 10^2$. Besides that, it is difficult to explain a wide range of the timescales met in a given pulsar.

These difficulties can be avoided if one take into account induced scattering inside the photon beam (Petrova 2004b). Let a narrow beam, with an opening angle $\Delta\theta \sim 1/\gamma$, propagate through the plasma flow at not a small angle to the magnetic field, $\theta \gg 1/\gamma$. The induced scattering acts mainly to redistribute the photon orientations inside the beam. The photons tend to be focused in the direction closest to the magnetic field direction.

Because of the focusing effect, the beam can be substantially squeezed, its angular width is now $\Delta\theta \sim 1/(\gamma\Gamma_b)$, where Γ_b is the optical depth to the scattering inside the beam. The observed timescales of microstructure require $\Gamma_b \sim 200$, which is consistent with the theoretical estimates of this quantity (Petrova 2004b). The focusing effect as a result of induced scattering not only removes the problem of exceedingly large Lorentz-factors of the plasma, but also explains a large scatter of the timescales observed in a given pulsar. This scatter is naturally attributed to the fluctuations in the plasma flow, in which case the scattering efficiency and the extent of focusing fluctuate as well. It is especially interesting to note that for a few pulsars studied the maximum observed scale of microstructure is compatible with the angular scale $\sim 1/\gamma$, which is indeed the case under condition of weak scattering, when $\Gamma_b \ll 1$.

The induced scattering inside the beam certainly holds during giant pulses, in addition to the beam-to-beam scattering which causes intensity amplification, and it is thought to be much more efficient because of the larger plasma densities and initial intensities peculiar to giant pulses. For the Crab pulsar we have the following estimates. The average optical depth to beam-to-beam scattering is $\langle\Gamma\rangle \sim 0.1$, whereas the maximum value $\Gamma_{\max} \approx 7$. As for the scattering inside the beam, $\langle\Gamma_b\rangle \sim 500$, and if this quantity can also increase by 70 times, the beam width is $\Delta\theta \sim 1/(70\langle\Gamma_b\rangle\gamma)$, which corresponds to the timescale $\Delta\tau = \Delta\theta P/(2\pi) \sim 10^{-9}$ s. Thus, the focusing effect as a result of induced scattering inside the beam can explain the structural details of giant pulses at timescales down to a nanosecond. Note that this interpretation naturally removes the problem of exceedingly high brightness temperatures of the nanopulses.

An idea of the focusing effect as the origin of the nanopulses finds a certain support in the observational plot of the peak intensities of the nanopulses versus their width, which has a clear upper envelope corresponding to the constant integrated intensity (Eilek et al. 2002). The points along the envelope can result from the focusing of different extent because of induced scattering inside the beam at different physical conditions, whereas the points below the envelope can correspond to different levels of true amplification due to the beam-to-beam scattering.

5 CONCLUSIONS

The main features of giant pulses and relative phenomena can be explained in terms of propagation effects in pulsar magnetosphere. Giant pulses can be caused by induced scattering in the flow of pulsar plasma. Induced scattering between substantially different frequencies and orientations leads to a marked redistribution of radio intensity in frequency. In the approximation of a superstrong magnetic field, the radio photons are mainly transferred from the lower-frequency state to the higher frequency one. With the decreasing spectrum of pulsar radiation, this may lead to a substantial increase of the higher-frequency intensity.

The optical depth to the beam-to-beam scattering is not large on average, but it depends on the plasma number density and the original radio intensity, which are believed to vary randomly from pulse to pulse. As from time to time they become larger than three times the average, the scattering depth becomes significant and amplification is efficient. Given that the plasma number density and the original intensity are Gaussian

random variables, the distribution of substantially amplified intensities is close to the power-law. Numerical simulations in the framework of the suggested model of intensity amplification allow to reproduce the observed intensity distributions of single pulses.

The mechanism suggested explains the location of giant pulses in the average pulse window in cases of the Crab and PSR B1937+21 and predicts strong polarization of giant emission in the plane of the ambient magnetic field. The nanostructure of giant pulses, as well as the microstructure of the normal ones, are explained by the focusing effect as a result of induced scattering inside the beam. The problem of exceedingly large brightness temperatures of the nanopulses is removed naturally.

Acknowledgements I am grateful to the Organizing Committee for the financial support which has made possible my participation in the Symposium. The work is in part supported by INTAS Grant No. 03-5727.

References

- Cairns I. H., Johnston S., Das P., 2001, *ApJ*, 563, L65
Eilek J. A., Arendt P. N., Hankins T. H., Weatherall J. C., 2002, in *Neutron Stars, Pulsars and SNRs*, ed. W. Backer, H. Lesch, J. Trumper, MPE Rep., No. 278, 249
Ershov A. A., Kuzmin A. D., 2003, *Astron. Lett.*, 29, 91
Hankins T. H., Kern J. S., Weatherall J. C., Eilek J. A., 2003, *Nature*, 422, 141
Johnston S., van Straten W., Kramer M., Bailes M., 2001, *ApJ*, 549, L101
Kramer M., Karastergiou A., Gupta Y. et al., 2003, *A&A*, 407, 655
Kuzmin A. D., Ershov A. A., Losovsky B. Ja., 2004, *Astron. Lett.*, 30, 247
Lundgren S. C., Cordes J. M., Ulmer M. et al., 1995, *ApJ*, 453, 433
Petrova S. A., 2004a, *A&A*, 424, 227
Petrova S. A., 2004b, *A&A*, 417, L29
Popov M. V., Bartel N., Cannon W. H. et al., 2002, *A&A*, 396, 171
Popov M. V., Stappers B., 2003, *Astron. Rep.*, 47, 660
Sallmen S., Backer D. C., Hankins T. H., Moffet D., Lundgren S., 1999, *ApJ*, 517, 460
Shearer A., Stappers B., Connor P. O., 2003, *Science*, 301, 493
Soglasnov V. A., Popov M. V., Bartel N. et al., 2004, *ApJ*, 616, 439